

Article

Dispersion Effects of Particulate Lead (Pb) from the Stack of a Lead Battery Recycling Plant

Dimitra Karali , Alexandros Stavridis , Glykeria Loupa  and Spyridon Rapsomanikis * 

Laboratory of Atmospheric Pollution and Pollution Control Engineering of Atmospheric Pollutants, Department of Environmental Engineering, School of Engineering, Democritus University of Thrace, 67100 Xanthi, Greece; dkarali@env.duth.gr (D.K.); stavridisa@gmail.com (A.S.); gloupa@env.duth.gr (G.L.)

* Correspondence: rapso@env.duth.gr; Tel.: +30-254-107-9380

Received: 23 September 2020; Accepted: 27 October 2020; Published: 30 October 2020



Abstract: The contribution of emissions from the stack of a lead battery recycling plant to atmospheric lead concentrations and, eventually, to the topsoil of the surrounding area, were studied. A Gaussian dispersion model, of the American Meteorological Society/United States Environmental Protection Agency Regulatory Model, (AERMOD) was used to determine atmospheric total suspended particulate lead dispersion, which originated from stack emissions, over the wider study area. Stack emission parameters were obtained from online measurements of the industry control sensors. AERMOD simulated two scenarios for four calendar years, 2015 to 2018, one for the typical stack measured operating conditions and one for the legal limit operating conditions (emissions from the stack set by legislation to 0.5 mg m^{-3}). Deposition fluxes modeled the input of atmospheric total suspended particulate Pb to the topsoil of the area. X-ray fluorescence (XRF) analyses were used to determine lead concentrations in the topsoil. The modeling results were compared with topsoil of six inhabited locations downwind from the stack in the direction of the prevailing winds to estimate the influence of lead deposition on topsoil near the industrial area.

Keywords: lead concentrations; lead battery recycling plant; AERMOD model; X-ray fluorescence (XRF)

1. Introduction

Lead is an environmentally persistent toxic metal. Even low levels of exposure can cause severe neurological damage that is sometimes irreversible [1,2]. It may be inhaled, ingested, or dermally absorbed. It is distributed to the brain, kidney, liver, and bones. It is stored in the bones and teeth, where it has an impact on human health. It affects the neurological, hematological, cardiovascular, gastrointestinal, and renal systems of humans. Infants, young children (especially those <5 years) and pregnant women are particularly vulnerable to the neurotoxic effects of Pb [3–6]. The increased environmental dispersion of lead is due to human activities, mainly from mining, smelting, and recycling of lead; production of lead-acid batteries and paints; electronic waste; and use in water pipes and solder [7]. Due to its persistence and global atmospheric transport, extraneous deposited lead can be detected even in remote regions of the world [8,9]. The widespread use of lead in the industrial era has resulted in extensive environmental and health problems in several parts of the world [10–13]. Lead occurs naturally in soil in small concentrations, mainly as lead sulfides, chlorides, or oxides [14], which originate from volcanic activity and sea spray terrestrial deposition.

AERMOD has been used extensively for the spatial dispersion of different pollutants originating from domestic landfills [15,16], a large industrial complex [17,18], and cities and counties [19–21]. Air pollutants' dispersion in the planetary boundary layer (PBL) may be described by a Gaussian

equation, which refers to steady state dispersion of air pollutants emitted by a continuous pollution source, such as a plume:

$$C(x, y, z, H) = \frac{Q}{2\pi\sigma_y\sigma_x u} \exp\left[-\frac{1}{2}\left(\frac{y}{\sigma_y}\right)^2\right] \left\{ \exp\left[-\frac{1}{2}\left(\frac{z-H}{\sigma_z}\right)^2\right] + \exp\left[-\frac{1}{2}\left(\frac{z+H}{\sigma_z}\right)^2\right] \right\} \quad (1)$$

where: C is the concentration at a point receptor, (g m^{-3}); (x, y, z) are surface coordinates of the receptor relative to the pollution source and the wind direction; H , height of pollutant's release, (m); Q , pollutant's exit flowrate, (g s^{-1}); u , wind direction, (m s^{-1}); σ_y , standard deviation of the plume concentration at y level, (m); σ_z , standard deviation of the plume concentration at z level, (m) [22–24]. AERMOD incorporates air dispersion based on the planetary boundary layer turbulence structure and scaling concepts, including treatment of both surface and elevated sources for both simple and complex terrain. The PBL is directly influenced by the Earth's surface in the form of frictional drag (from topology and obstacles such as buildings, etc.), solar heating (radiation), and evapotranspiration. Most pollutants are released in this layer, and its temperature and turbulent structure is highly important for short range pollutant transport. From the mathematical (modeling) perspective, the dispersion of air pollutants is described by the above Gaussian equation for a steady state emission of pollutants from a stationary source.

The present study investigates the effect of atmospheric emissions from a lead battery recycling plant on recipients within a 15 km distance from the plant. The major concern that arises from the operation of the plant is the effect of the stack emissions on the surrounding inhabited area. This concern is associated with the annual average particulate lead atmospheric concentrations and the topsoil burden of lead from its deposition. The AERMOD model calculates the concentrations of dispersed particulate lead (Pb) at any chosen recipient position in a 20×20 km grid, at 10 m height, and at a one hour time interval and 100 m spatial resolution. These modelling results were obtained for the four calendar years of 2015 to 2018. The model was run hourly for four calendar years, for two scenarios of Pb emissions: (a) the typical recorded operating stack emissions from the recycling plant and (b) the hypothetical case of the legal limit operating conditions. The EU legislation enforces the limits of the annual average concentration levels arriving at the recipient. These concentrations were calculated for each of the 72 local settlements (hamlets, villages, towns) that can be found in the grid under study. The highest hourly atmospheric concentrations of total suspended particulate (TSP) of Pb arriving at the 72 recipient settlements per year were also calculated for the period of four years. These were extracted from 8760 hourly calculations (one hour time resolution for one year) for 40,401 grid points (201×201 grid points for a $20 \text{ km} \times 20 \text{ km}$ grid with 100 m spatial resolution) using meteorological data obtained from the AERMOD hub. Hence there were 353,912,760 calculated results per year per scenario. It also follows that these data were used to obtain the mean annual values at each of the 72 recipients and compare them with the prevailing legislation. Lead in the soil should be kept at the lowest levels possible to prevent consequent increases in the exposure of humans and the biome. For this reason, the present study estimates the theoretical increase in lead concentration in topsoil for two different deposition velocities of particles. Concentration levels of Pb in topsoil were determined in six locations near the industrial area. Specific soil limit values for lead differ according to state and protection agency. However, typical hand-to-mouth behavior of children with regard to soil suggests Pb-laden topsoil is a potentially serious source of exposure.

2. Materials and Methods

2.1. Study Area

This study was carried out in the industrial area of Komotini, Northern Greece. The lead battery recycling plant operating in Komotini mainly recycles industrial fork-lift batteries, uninterruptable power supply (UPS) batteries, and car and motorcycle batteries. The efficiency of the Air Pollution Control System of this lead battery recycling plant was presented in a previous study [2].

More specifically, the suspended particles in the stack from April 2018 to 21 June 2018 were measured with a laser dust monitor (NEOM, NEO Monitors AS, Skedsmokorset, Norway). This is an optical instrument based on transmitting a visible laser light from a transmitter unit on one side of the stack to a receiver on the diametrically opposite side of the stack. The measuring technique is based on measuring absorption and the scattering of light created by the dust particles present in the stack. The measurement signal corresponds to the integrated dust concentration over the entire optical stack path.

Figure 1 depicts the recipients located less than 15 km from factory stack.

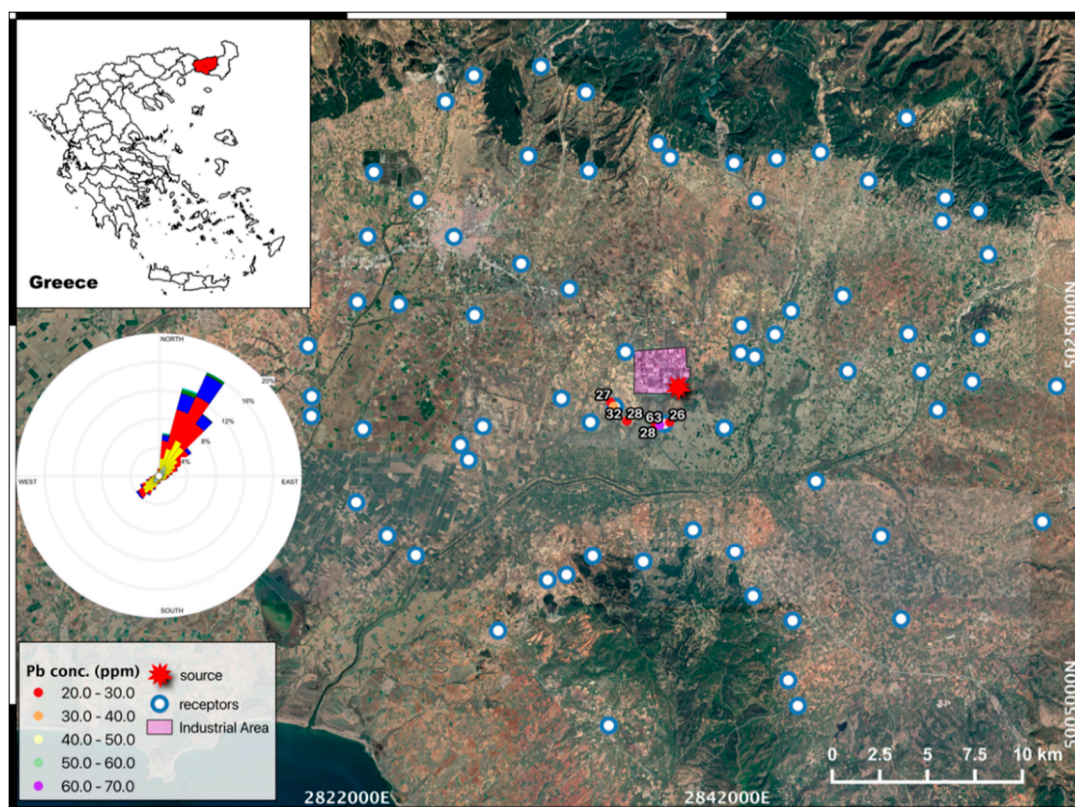


Figure 1. Study area with 72 discrete receptors and the source. Insert lists lead concentration detected in the topsoil of six locations.

2.2. Dispersion Modelling

AERMOD [25] is a regulatory steady-state Gaussian plume model (Lakes Environmental Software, Waterloo, ON, Canada). The “steady state” refers to meteorological condition of “steady” for at least one hour. Hence, the meteorological parameters for 8760 h per year were used. Input files for the AERMOD, for the Industrial Source Complex Short Term Version 3 (ISCST3), for the Agency Regulatory Model Improvement Committee (AERMIC), and the Environmental Protection Agency (EPA) regulatory models originate from the AERMOD Meteorological Preprocessor (AERMET) and the AERMOD Terrain Preprocessor AERMAP [26]. Specifically, AERMET uses meteorological data and surface characteristics to calculate boundary layer and micrometeorological parameters (e.g., mixing height and friction velocity) necessary for the AERMOD calculations. AERMAP uses gridded terrain data for the modeling area to calculate a representative terrain-influenced height associated with each receptor location. At the present time, the gridded data of AERMAP are supplied by a digital elevation model (DEM) data. AERMET uses meteorological data, representative of the modeling domain, to compute and estimate height profiles of wind, turbulence, and temperature. The study area has its own “fetch” characteristics (e.g., contour, elevation, land use, vegetation). In addition to planetary

boundary layer (PBL) parameters, AERMOD obtains data for wind, temperature, and turbulence in its required form, from AERMET.

2.2.1. Meteorological Data

Data were purchased from the AERMOD service hub. The MM5 (5th generation Mesoscale National Center for Atmospheric Research Model) output files are converted into a format recognized by the AERMET model (meteorological preprocessor for AERMOD). The final output was generated by creating a pseudo met-station at the location of the stack of the lead battery recycling plant.

2.2.2. Receptors

All towns, villages, and hamlets located less than 15 km from the stack were considered receptors. A uniform Cartesian grid of 20×20 km with 100 m spacing was used to estimate the spatial extent of elevated Pb concentrations near the industrial area of Komotini. The receptors are shown in Figure 1.

2.2.3. Stack Operation Parameters

Emissions from the stack of the lead battery recycling plant are the source of the pollutant dispersion. The stack emission characteristics are tabulated below in Table 1. This study investigated two scenarios for each year in the period 2015–2018. In the first scenario the recorded operating conditions of the plant were studied, whereas in the second scenario the legal limit operating conditions of the plant were used. In the first scenario it was assumed that the plant emitted a constant $0.0036 \text{ mg Pb m}^{-3}$ [2]. In the legal limit operating conditions, the dispersion of lead was modeled using AERMOD, in which it was assumed that the plant emitted 0.5 mg Pb m^{-3} , i.e., the upper limit set by the EU legislation [27].

Table 1. Source parameters.

Scenario	Typical Operating Conditions	Legal Limit Operating Conditions
Source		Point
X (UTM35)		374555.62
Y (UTM35)		4546885.51
Height (m)		19.7 m
Diameter (m)		2.5 m
Stack exit gas temperature ($^{\circ}\text{C}$)		80 $^{\circ}\text{C}$
Gas exit flow rate ($\text{m}^3 \text{ s}^{-1}$)		44.4 $\text{m}^3 \text{ s}^{-1}$
Gas exit velocity (m s^{-1})		9.053 m s^{-1}
Emission rates of the Pb particulate matter (g s^{-1})	0.00016 g s^{-1}	0.0222 g s^{-1}

2.3. Topsoil

To estimate the influence of lead emissions on topsoil near the industrial area, elemental analysis of the soil for background observations was carried out and the future increase in lead concentration in the topsoil was calculated.

2.3.1. Elemental Analysis

For the elemental analysis of topsoil, X-ray fluorescence spectroscopy (XRF) was used. This technique was selected because it allows the simultaneous analysis of several elements and does not destroy the samples [28,29]. Six topsoil samples were collected from the study area. The sampling points are shown in Figure 1. Pellets were analyzed by a wavelength dispersive X-ray fluorescence system (WDXRF, Rigaku, ZSX Primus II, Tokyo, Japan). Forty elements were detected and quantified to study the footprint of the area and possible effect of the plant. The detection limit for lead was

3.6 ppm. Our results were then compared to the Forum of European Geological Surveys (FOREGS) maps [30].

2.3.2. Influence of Lead Emissions on Topsoil

To calculate lead concentration in the soil due to plant operation, some assumptions were made. Based on the air mass concentration of lead (C_{Pb}) determined by AERMOD, and assuming two different deposition velocities of particles ($\mu\text{g s}^{-1}$), the mass flux density was calculated (F , the rate of mass flux per unit area) using the equation:

$$F = u_g \cdot C_{Pb}, \quad (2)$$

The deposition velocities on soil may differ by three orders of magnitude for particles [31]. Hence, the value of 0.008 cm s^{-1} was used, as given by Little and Wiffen [32] for Pb auto exhaust as the depositing material. A value of 0.36 cm s^{-1} , provided by Creclius [33], was used for the atmospheric aggregates depositing on soil. Hence, the percentage estimation of topsoil future loads based on background values as determined by X-ray fluorescence were calculated based on two assumed deposition velocities of particles and one topsoil density. For the study area the topsoil density given by the Land Cover/Use Statistics (LUCAS) database was considered to be 1600 kg m^{-3} [34].

3. Results

3.1. AERMOD Dispersion Results

Figures 2 and 3 show the annual average concentration of total suspended particulate (TSP) of Pb ($\mu\text{g m}^{-3}$) in the lower atmosphere for each scenario per year. European legislation sets the threshold of Pb at $0.5 \mu\text{g m}^{-3}$ mean concentration for a calendar year [35]. Figure 4 shows the annual average concentration of TSP of Pb ($\mu\text{g m}^{-3}$) for 72 receptors for each scenario per year. As shown in Table S1, Amaranta has the highest annual values of the area for both scenarios and years.

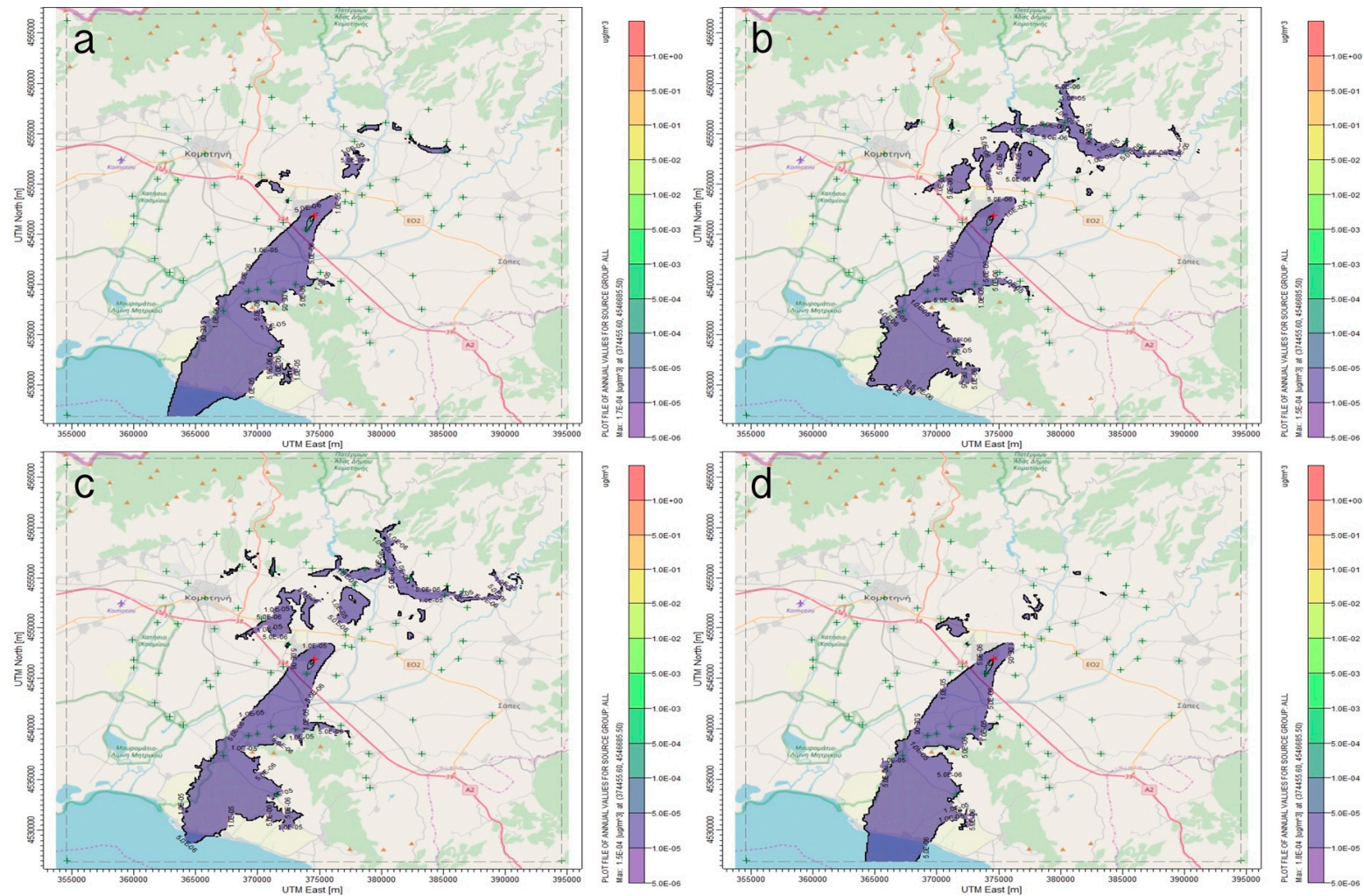


Figure 2. Annual average concentration of TSP of Pb ($\mu\text{g m}^{-3}$) for (a) the typical operating conditions for 2015, (b) the typical operating conditions for 2016, (c) the typical operating conditions for 2017, and (d) the typical operating conditions for 2018.

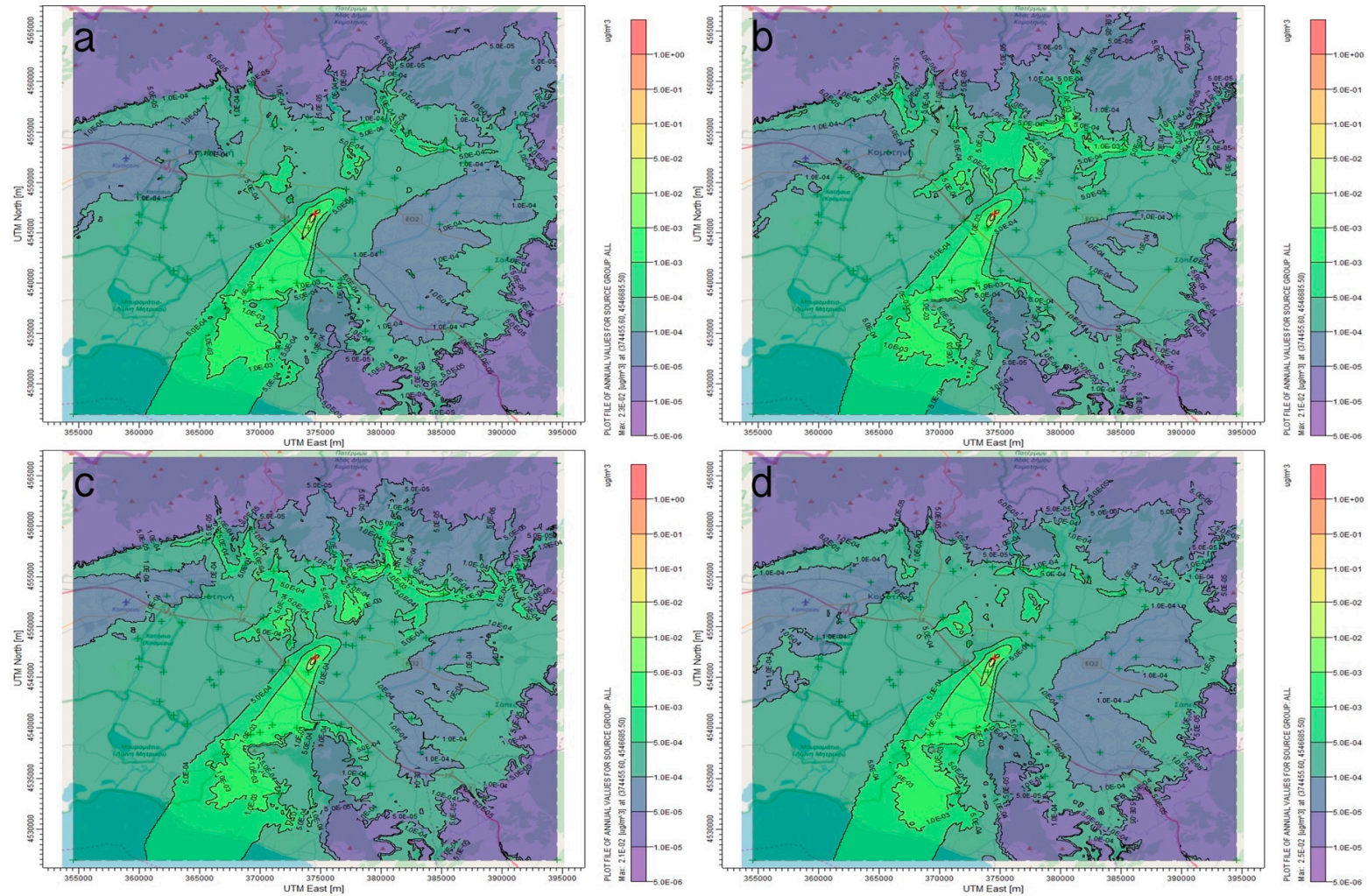


Figure 3. Annual average concentration of TSP of Pb ($\mu\text{g m}^{-3}$) for (a) the legal limit operating conditions for 2015, (b) the legal limit operating conditions for 2016, (c) the legal limit operating conditions for 2017, and (d) the legal limit operating conditions for 2018.

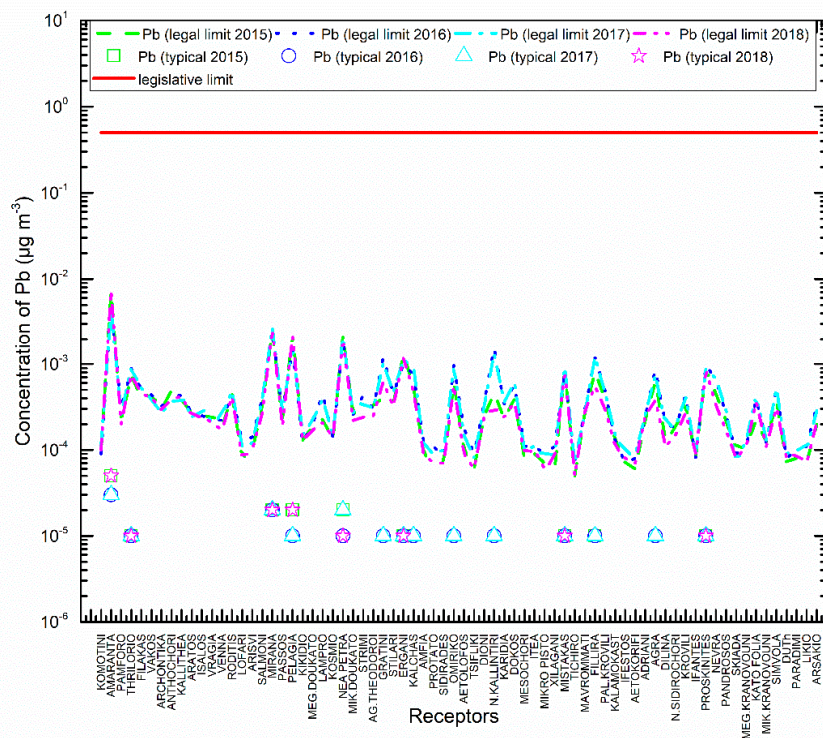


Figure 4. Annual average concentration of Pb ($\mu\text{g m}^{-3}$) for 72 receptors compared to the annual legislation limit of $0.5 \mu\text{g m}^{-3}$.

To estimate the burden on the recipients we calculated the maximum hourly values. The highest hourly concentrations of Pb “observed” at the recipients is $3.32 \times 10^{-3} \mu\text{g m}^{-3}$ for 20 hours for the “typical operating conditions” and $0.461 \mu\text{g m}^{-3}$ for the “legal limit operating conditions” for 20 h in Fillira both on 4 June 2016 (Figures 5 and 6 and Table S2).

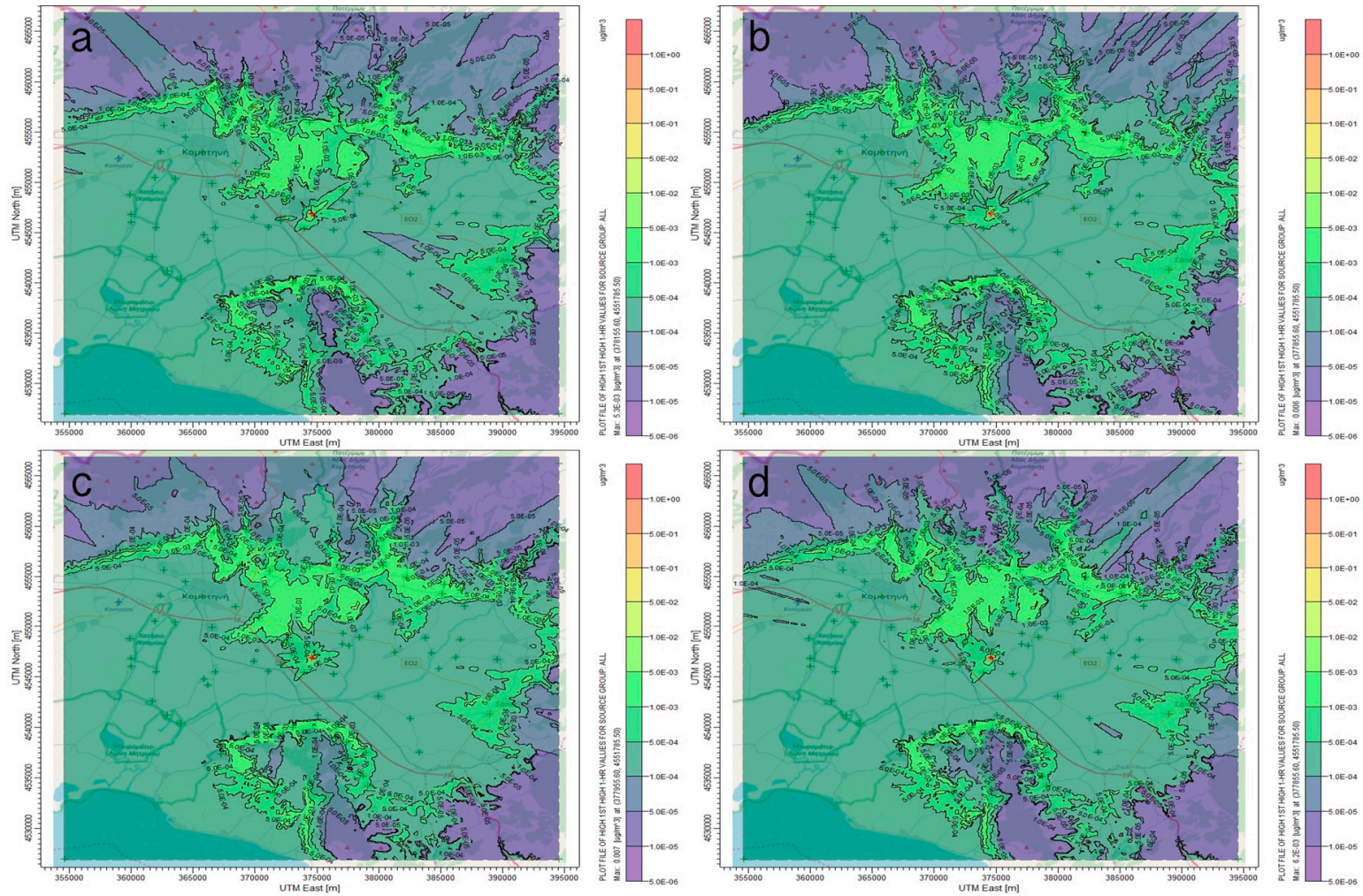


Figure 5. The highest hourly values of TSP of Pb ($\mu\text{g m}^{-3}$) (a) the typical operating conditions for 2015, (b) the typical operating conditions for 2016, (c) the typical operating conditions for 2017, and (d) the typical operating conditions for 2018.

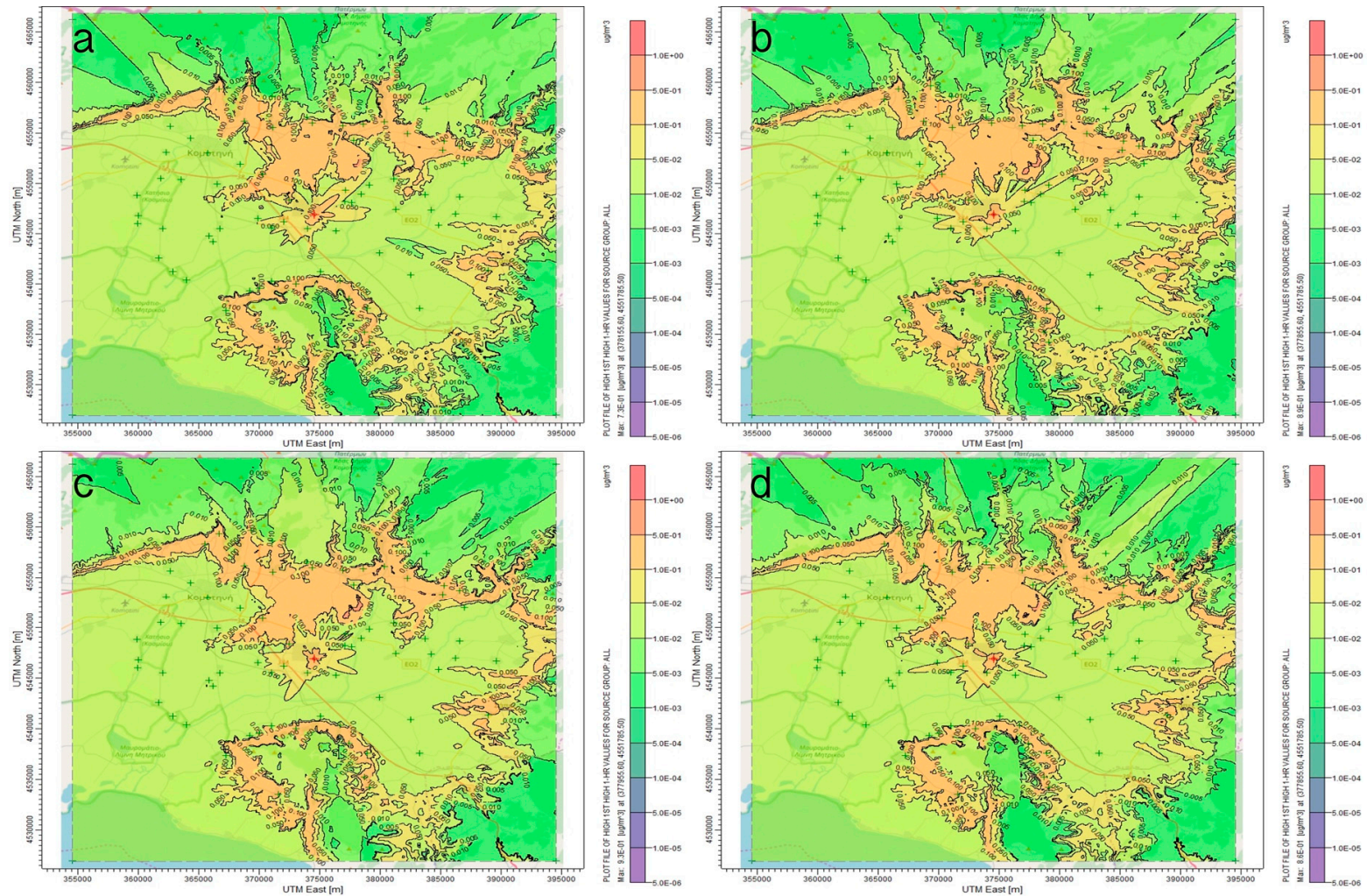


Figure 6. The highest hourly values of TSP of Pb ($\mu\text{g m}^{-3}$) (a) the legal limit operating conditions for 2015 (b) the legal limit operating conditions for 2016, (c) the legal limit operating conditions for 2017, and (d) the legal limit operating conditions for 2018.

3.2. Influence of Stack Emissions on the Topsoil of the Area

Amaranta and Filakas villages were selected for soil sampling collection because these regions have the greatest deposition burden in the industrial area. These are located to the south of the industrial area of Komotini, where the prevailing wind originates from the north or north-east. Six samples were collected in which topsoil lead concentrations were between 27 and 32 ppm. However, one outlier at 63 ppm existed because that sample was taken near a bus station in Amaranta. The results are similar to those indicated by the FOREGS maps, where topsoil lead concentrations have indicative values of 28–35 ppm (mg kg^{-1}) [36]. It is also assumed that, in the calculations below, the only input to the topsoil originates from the TSP of Pb of the battery recycling factory. This assumption may be not true because there may be other sources of deposition to the topsoil. In the present case, the effect of the contribution of the TSP of Pb from the battery recycling factory on the topsoil is calculated.

Two different scenarios for calculating the topsoil deposition burden were carried out based on two deposition velocities, namely 0.008 and 0.36 cm s^{-1} . Hence, the mass flux was 0.015 and $0.681 \text{ mg m}^{-2} \text{ year}^{-1}$ for the two deposition velocity values, respectively, and the four year mean of 6 ng m^{-3} atmospheric lead concentration in Amaranta was taken into account:

- Scenario 1

From AERMOD for Amaranta, four year mean lead concentration: $0.006 \text{ } \mu\text{g m}^{-3}$

Deposition velocity: 0.00008 m s^{-1} . As calculated below, mass flux = $0.0151 \text{ mg m}^{-2} \text{ year}^{-1}$:

$$\begin{aligned} F &= 0.006 \frac{\text{ug}}{\text{m}^3} \cdot 0.00008 \frac{\text{m}}{\text{s}} = 5.28 \cdot 10^{-7} \frac{\text{ug}}{\text{m}^2\text{s}} \\ &= 5.28 \cdot 10^{-7} \frac{\text{ug}}{\text{m}^2\text{s}} \cdot 86,400 \frac{\text{s}}{\text{day}} \cdot 360 \frac{\text{day}}{\text{year}} \\ F &= 15.14 \frac{\text{ug}}{\text{m}^2\text{year}} = 0.015 \frac{\text{mg}}{\text{m}^2\text{year}} \end{aligned}$$

Assuming that the topsoil has a depth of 0.1 m and density 1600 kg m^{-3} :

$$\begin{aligned} F &= 15.14 \frac{\text{ug}}{\text{m}^2\text{year}} = 0.015 \frac{\text{mg}}{\text{m}^2\text{year}} \\ \frac{0.15 \frac{\text{mg}}{\text{m}^3\text{year}}}{1600 \frac{\text{kg}}{\text{m}^3}} &= 9.46 \cdot 10^{-5} \frac{\text{mg}}{\text{kg year}} \end{aligned}$$

For the topsoil to reach the European legislative limit of 50 ppm from the detected 25 ppm and assuming that the only Pb to topsoil input originates from the factory stack emissions, the required number of years is $264,248$:

$$\frac{25 \frac{\text{mg}}{\text{kg}}}{9.46 \cdot 10^{-5} \frac{\text{mg}}{\text{kg year}}} = 264,248 \text{ years}$$

This also means a percentage loading per year of 0.00038% .

- Scenario 2

From AERMOD for Amaranta, four year mean lead concentration: $0.006 \text{ } \mu\text{g m}^{-3}$.

Deposition velocity: $0.36 \text{ cm s}^{-1} = 0.0036 \text{ m s}^{-1}$. As calculated below, mass flux = $0.681 \text{ mg m}^{-2} \text{ year}^{-1}$:

$$\begin{aligned} F &= 0.006 \frac{\mu\text{g}}{\text{m}^3} \cdot 0.0036 \frac{\text{m}}{\text{s}} = 2.16 \cdot 10^{-5} \frac{\mu\text{g}}{\text{m}^2\text{s}} \\ &= 2.16 \cdot 10^{-5} \frac{\mu\text{g}}{\text{m}^2\text{s}} \cdot 86,400 \frac{\text{s}}{\text{day}} \cdot 360 \frac{\text{day}}{\text{year}} \\ F &= 681.2 \frac{\mu\text{g}}{\text{m}^2\text{year}} = 0.681 \frac{\text{mg}}{\text{m}^2\text{year}} \end{aligned}$$

Assuming that the topsoil has a depth of 0.1 m and a density of 1600 kg m^{-3} :

$$\begin{aligned} \frac{0.681 \frac{\text{mg}}{\text{m}^2\text{year}}}{0.1\text{m}} &= 6.81 \frac{\text{mg}}{\text{m}^3\text{year}} \\ \frac{6.81 \frac{\text{mg}}{\text{m}^3\text{year}}}{1600 \frac{\text{kg}}{\text{m}^3}} &= 4.26 \cdot 10^{-3} \frac{\text{mg}}{\text{kg year}} \end{aligned}$$

For the topsoil to reach the European legislative limit of 50 ppm from the detected 25 ppm and assuming that the only input Pb to the topsoil originates from the factory stack emissions, the required number of years is 5872:

$$\frac{25 \frac{\text{mg}}{\text{kg}}}{4.26 \cdot 10^{-3} \frac{\text{mg}}{\text{kg year}}} = 5872 \text{ years}$$

This also means a percentage loading per year of 0.017%.

4. Discussion

The annual, dispersed average mass concentrations of Pb ($\mu\text{g m}^{-3}$) for the four years and for the two stack emission scenarios are depicted in Figures 2 and 3. The maxima never reach $0.5 \mu\text{g m}^{-3}$ at any point over the four year period in the dispersion modeled area. Thus, the values never exceeded the annual limit as also shown in Figure 4. The highest annual values on the receptors were observed in Amaranta for both scenarios and years. However, when calculated as a percentage of the limits set by legislation, these only equated to 0.006% ($3.00 \times 10^{-5} \mu\text{g m}^{-3}$ in 2015 and 2018) and 1.458% ($7.29 \times 10^{-3} \mu\text{g m}^{-3}$ in 2018) for the typical operating conditions and legal limit operating conditions, respectively.

The average mass concentrations of lead in airborne particles are usually below $0.15 \mu\text{g m}^{-3}$ at nonurban sites and typically between 0.15 and $0.5 \mu\text{g m}^{-3}$ in urban areas [37–39]. The mass concentration of lead in aerosols in Greek sites ranges from 5.69 to 39.4 ng m^{-3} [40–44] for coarse particles and 4.1 to 42 ng m^{-3} for fine particles [42,45–47]. All of the above monitoring studies were carried out after 2000, which was the last year in which it was permitted to use gasoline with lead additives. The deadline for Greece was extended until 2001. The increase in atmospheric lead levels from the stack was 0.53% (0.03 ng m^{-3} at 5.69 ng m^{-3}) and 128.12% (7.29 ng m^{-3} at 5.69 ng m^{-3}) for the two scenarios, respectively. The percentage variation was calculated based on the minimum atmospheric lead concentrations in Greek cities for coarse particles.

To estimate the influence of lead deposition on topsoil near the industrial area, the annual topsoil burden of Pb was calculated. The Pb limit in soil is 50–300 ppm (mg kg^{-1}) [48] and the limit value proposed by the Joint Research Centre (JRC) is 50 mg kg^{-1} [49]. Hence, the contribution of TSP Pb from the stack to the Pb topsoil burden, is 0.00038% under the usual operating conditions, and 0.017% for the legal limit operating conditions scenario. Assuming that the lead recycling plant stack is the

only lead contributor to the topsoil, it would take thousands of years (calculated above) for the lead concentration of the topsoil to reach the legislation limit, i.e., from ca. 25 ppm to 50 ppm. Hence, the influence of lead stack emissions from the plant to the topsoil near the industrial area is negligible.

5. Conclusions

The main concern of the study was the influence of stack emissions of TSP of lead on the atmosphere and topsoil of the local habitable areas. Dispersion modeling for TSP lead (Pb) originating from the typical operation of a lead recycling plant was carried out in its vicinity (a grid of 20 × 20 km). Modeling for the same pollutant was also carried out for the hypothetical conditions under which stack emissions reached emission limits set by the EU. The regulatory model AERMOD was used in this modeling and all results were compared to the annual limit concentration values arriving at 72 receptors. In conclusion, the dispersed pollutants arriving at the recipients reached concentration values of only a few percent of the above regulatory annual limit values and under no circumstance threatened humans or the biome. Furthermore, the deposition of particulate lead from these emissions does not constitute a serious burden to the local topsoil.

Supplementary Materials: The following are available online at <http://www.mdpi.com/1996-1073/13/21/5690/s1>, Table S1: Annual average concentrations of Pb arriving at the 72 discrete residential areas in the region of study for two scenarios, Table S2: Highest hourly values of Pb arriving at the 72 discrete residential areas in the region of study for two scenarios.

Author Contributions: Conceptualization, S.R. and G.L.; methodology, D.K. and A.S.; software, D.K.; data curation, D.K. and A.S.; writing—original draft preparation, D.K.; writing—review and editing, S.R. and G.L.; supervision, S.R. All authors have read and agreed to the published version of the manuscript.

Funding: This research received no external funding.

Acknowledgments: Thanks are due to the “SUNLIGHT S.A.” factory administration for allowing access to their premises and their emission data.

Conflicts of Interest: The authors declare no conflict of interest.

References

1. International Programme for Chemical Safety. *Inorganic Lead*; World Health Organization: Geneva, Switzerland, 1995.
2. Kelektoglou, K.; Karali, D.; Stavridis, A.; Loupa, G. Efficiency of the Air-Pollution Control System of a Lead-Acid-Battery Recycling Industry. *Energies* **2018**, *11*, 3465. [[CrossRef](#)]
3. Eguchi, A.; Nomiya, K.; Sakurai, K.; Trang, P.T.K.; Viet, P.H.; Takahashi, S.; Iwata, H.; Tanabe, S.; Todaka, E.; Mori, C. Alterations in urinary metabolomic profiles due to lead exposure from a lead-acid battery recycling site. *Environ. Pollut.* **2018**, *242*, 98–105. [[CrossRef](#)] [[PubMed](#)]
4. Risk Assessment Guidance for Superfund. *Volume I: Human Health Evaluation Manual (Part A)*; EPA/540/1-89/002; Environmental Protection Agency: Washington, DC, USA, 1989.
5. Järup, L. Hazards of heavy metal contamination. *Br. Med. Bull.* **2003**, *68*, 167–182. [[CrossRef](#)] [[PubMed](#)]
6. WHOQOL Group. WHO, The World Health Organization quality of life assessment (WHOQOL): Position paper from the World Health Organization. *Soc. Sci. Med.* **1995**, *41*, 1403–1409. [[CrossRef](#)]
7. UNEP. Draft final review of scientific information on lead. In *United Nations Environment Programme, Chemicals Branch*; UNEP: Nairobi, Kenya, 2008.
8. Johansson, K.; Bergbäck, B.; Tyler, G. Impact of Atmospheric Long Range Transport of Lead, Mercury and Cadmium on the Swedish Forest Environment. *Water Air Soil Pollut. Focus* **2001**, *1*, 279–297. [[CrossRef](#)]
9. Health risks of heavy metals from long-range transboundary air pollution. In *World Health Organization Regional Office for Europe*; WHO: Geneva, Switzerland, 2007.
10. Collivignarelli, C.; Riganti, V.; Urbini, G. Battery lead recycling and environmental pollution hazards. *Conserv. Recycl.* **1986**, *9*, 111–125. [[CrossRef](#)]
11. Ettler, V.; Johan, Z.; Baronnet, A.; Jankovský, F.; Gilles, C.; Mihaljevič, M.; Šebek, O.; Strnad, L.; Bezdička, P. Mineralogy of air-pollution-control residues from a secondary lead smelter: Environmental implications. *Environ. Sci. Technol.* **2005**, *39*, 9309–9316. [[CrossRef](#)]

12. Milton, B.-A.; Juan, V.M.; María, M.V.; Alejandro, A.; José, P.-C.J. Chemical characterization and local dispersion of slag generated by a lead recovery plant in Central Mexico. *Afr. J. Biotechnol.* **2014**, *13*, 1973–1978.
13. Salomone, R.; Mondello, F.; Lanuzza, F.; Micali, G. An eco-balance of a recycling plant for spent lead–acid batteries. *Environ. Manag.* **2005**, *35*, 206–219. [[CrossRef](#)]
14. IARC. Summaries & evaluations: Inorganic and organic lead compounds. In *International Agency for Research on Cancer (IARC Monographs for the Evaluation of Carcinogenic Risks to Humans)*; IARC: Lyon, France, 2006; Volume 87.
15. Araiza-Aguilar, J.A.; Rojas-Valencia, M.N. Spatial modelling of gaseous emissions from two municipal solid waste dump sites. *Int. J. Environ. Stud.* **2019**, *76*, 213–224. [[CrossRef](#)]
16. Maticchiera, F.; Manes, C.; Beaven, R.P.; Rees-White, T.C.; Boano, F.; Mønster, J.; Scheutz, C. AERMOD as a Gaussian dispersion model for planning tracer gas dispersion tests for landfill methane emission quantification. *Waste Manag.* **2019**, *87*, 924–936. [[CrossRef](#)] [[PubMed](#)]
17. Abril, G.A.; Diez, S.C.; Pignata, M.L.; Britch, J. Particulate matter concentrations originating from industrial and urban sources: Validation of atmospheric dispersion modeling results. *Atmos. Pollut. Res.* **2016**, *7*, 180–189. [[CrossRef](#)]
18. Dos Santos Cerqueira, J.; de Albuquerque, H.N.; de Assis Salviano de Sousa, F. Atmospheric pollutants: Modeling with Aermod software. *Air Qual. Atmos. Health* **2019**, *12*, 21–32. [[CrossRef](#)]
19. Gibson, M.D.; Kundu, S.; Satish, M. Dispersion model evaluation of PM_{2.5}, NO_x and SO₂ from point and major line sources in Nova Scotia, Canada using AERMOD Gaussian plume air dispersion model. *Atmos. Pollut. Res.* **2013**, *4*, 157–167. [[CrossRef](#)]
20. Macêdo, M.F.M.; Ramos, A.L.D. Vehicle atmospheric pollution evaluation using AERMOD model at avenue in a Brazilian capital city. *Air Qual. Atmos. Health* **2020**, *13*, 309–320. [[CrossRef](#)]
21. Makridis, M.; Lazaridis, M. Dispersion modeling of gaseous and particulate matter emissions from aircraft activity at Chania Airport, Greece. *Air Qual. Atmos. Health* **2019**, *12*, 933–943. [[CrossRef](#)]
22. De Nevers, N. *Air Pollution Control Engineering*; Waveland Press: Long Grove, IL, USA, 2010.
23. Dornbrack, A. *Turbulence and diffusion in the atmosphere Lectures in Environmental Sciences*; Blackadar, A.K., Ed.; Springer-Verlag GmbH & Co. KG: Berlin/Heidelberg, Germany, 1997; p. 185. ISBN 3540- 61406-0.
24. Turner, D.B. *Workbook of Atmospheric Dispersion Estimates: An Introduction to Dispersion Modeling*; CRC Press: Boca Raton, FL, USA, 1994.
25. EPA. AERMOD Implementation Guide. In *Aermod Implementation Workgroup, U.S. Environmental Protection Agency, Office of Air Quality Planning and Standards*; Air Quality Assessment Division: North Carolina, NC, USA, 2009.
26. EPA. AERMOD: Description of Model Formulation. In *On Assignment to the Atmospheric Research And Exposure Assessment Laboratory, U.S. Environmental Protection Agency*; EPA-454/R-03-004 September 2004; U.S. Environmental Protection Agency, Office of Air Quality Planning and Standards, Emissions Monitoring and Analysis Division: North Carolina, NC, USA, 2004.
27. Directive 2010/75/EU of the European Parliament and of the Council of 24 November 2010 on industrial emissions (integrated pollution prevention and control). *Off. J. Eur. Union L* **2010**, *334*, 17–119.
28. Brouwer, P. *Theory of XRF: Getting Acquainted with the Principles*; PANalytical BV: Almelo, The Netherlands, 2006.
29. Jaklevic, J. *Photon Induced X-ray Fluorescence Analysis Using Energy Dispersive Detector and Dichotomous Sampler*; Lawrence Berkeley Laboratory University of California: Berkeley, CA, USA, 1976.
30. Tarvainen, T.; Reeder, S.; Albanese, S. Database management and map production. *Geochem. Atlas Eur. Part* **2005**, *1*, 526.
31. Sehmel, G.A. Particle and gas dry deposition: A review. *Atmos. Environ. (1967)* **1980**, *14*, 983–1011. [[CrossRef](#)]
32. Little, P.; Wiffen, R. Emission and deposition of petrol engine exhaust Pb—I. Deposition of exhaust Pb to plant and soil surfaces. *Atmos. Environ. (1967)* **1977**, *11*, 437–447. [[CrossRef](#)]
33. Crecelius, E.; Robertson, D.; Abel, K.; Cochran, D.; Weimer, W. Atmospheric deposition of ⁷Be and other elements on the Washington coast. In *Pacific Northwest Laboratory Annual Report for 1977 to the DOE Assistant Secretary for Environment: Ecological Sciences*; PNL-2500 PT 2; Pacific Northwest Laboratory Richland: Richland, WA, USA, 1978; pp. 983–1011.
34. Ballabio, C.; Panagos, P.; Monatanarella, L. Mapping topsoil physical properties at European scale using the LUCAS database. *Geoderma* **2016**, *261*, 110–123. [[CrossRef](#)]

35. Directive 2008/50/EC of the European Parliament and of the Council of 21 May 2008 on ambient air quality and cleaner air for Europe. *Off. J. Eur. Union* **2008**.
36. Lado, L.R.; Hengl, T.; Reuter, H.I. Heavy metals in European soils: A geostatistical analysis of the FOREGS Geochemical database. *Geoderma* **2008**, *148*, 189–199. [[CrossRef](#)]
37. Del Delumyea, R.; Kalivretenos, A. Elemental carbon and lead content of fine particles from American and French cities of comparable size and industry, 1985. *Atmos. Environ. (1967)* **1987**, *21*, 1643–1647. [[CrossRef](#)]
38. Frank, J.J.; Poulakos, A.G.; Tornero-Velez, R.; Xue, J. Systematic review and meta-analyses of lead (Pb) concentrations in environmental media (soil, dust, water, food, and air) reported in the United States from 1996 to 2016. *Sci. Total Environ.* **2019**, *694*, 133489. [[CrossRef](#)] [[PubMed](#)]
39. *Air Quality Guidelines for Europe*; WORLD HEALTH ORGANIZATION: Geneva, Switzerland, 2000.
40. Diapouli, E.; Manousakas, M.; Vratolis, S.; Vasilatou, V.; Maggos, T.; Saraga, D.; Grigoratos, T.; Argyropoulos, G.; Voutsas, D.; Samara, C.; et al. Evolution of air pollution source contributions over one decade, derived by PM₁₀ and PM_{2.5} source apportionment in two metropolitan urban areas in Greece. *Atmos. Environ.* **2017**, *164*, 416–430. [[CrossRef](#)]
41. Grigoratos, T.; Samara, C.; Voutsas, D.; Manoli, E.; Kouras, A. Chemical composition and mass closure of ambient coarse particles at traffic and urban-background sites in Thessaloniki, Greece. *Environ. Sci. Pollut. Res.* **2014**, *21*, 7708–7722. [[CrossRef](#)]
42. Karageorgos, E.; Rapsomanikis, S. *Chemical Characterization of the Inorganic Fraction of Aerosols and Mechanisms of the Neutralization of Atmospheric Acidity in Athens, Greece*; Copernicus Publications on behalf of the European Geosciences Union; Copernicus Publications: Göttingen, Germany, 2007.
43. Manoli, E.; Chelioti-Chatzidimitriou, A.; Karageorgou, K.; Kouras, A.; Voutsas, D.; Samara, C.; Kampanos, I. Polycyclic aromatic hydrocarbons and trace elements bounded to airborne PM₁₀ in the harbor of Volos, Greece: Implications for the impact of harbor activities. *Atmos. Environ.* **2017**, *167*, 61–72. [[CrossRef](#)]
44. Terzi, E.; Argyropoulos, G.; Bougatioti, A.; Mihalopoulos, N.; Nikolaou, K.; Samara, C. Chemical composition and mass closure of ambient PM₁₀ at urban sites. *Atmos. Environ.* **2010**, *44*, 2231–2239. [[CrossRef](#)]
45. Grivas, G.; Cheristanidis, S.; Chaloulakou, A.; Koutrakis, P.; Mihalopoulos, N. Elemental Composition and Source Apportionment of Fine and Coarse Particles at Traffic and Urban Background Locations in Athens, Greece. *Aerosol Air Qual. Res.* **2018**, *18*, 1642–1659. [[CrossRef](#)]
46. Remoundaki, E.; Kassomenos, P.; Mantas, E.; Mihalopoulos, N.; Tsezos, M. Composition and Mass Closure of PM_{2.5} in Urban Environment (Athens, Greece). *Aerosol Air Qual. Res.* **2013**, *13*, 72–82. [[CrossRef](#)]
47. Theodosi, C.; Tsagkaraki, M.; Zarmpas, P.; Grivas, G.; Liakakou, E.; Paraskevopoulou, D.; Lianou, M.; Gerasopoulos, E.; Mihalopoulos, N. Multi-year chemical composition of the fine-aerosol fraction in Athens, Greece, with emphasis on the contribution of residential heating in wintertime. *Atmos. Chem. Phys.* **2018**, *18*, 14371–14391. [[CrossRef](#)]
48. Directive 86/278/EEC of 12 June 1986. Protection of the Environment, and in Particular of the Soil, When Sewage Sludge is Used in Agriculture. 1986. Available online: <http://gov.wales/topics/environmentcountryside/farmingandcountryside/farming/farm-regulations-wales/farmregs-wales-waste/directive-86-278-eec-sewage-sludgesoil> (accessed on 20 September 2020).
49. Langenkamp, H.; für Geowissenschaften, B.; Düwel, O.; Utermann, J. Progress Report Trace Element and Organic Matter Contents of European Soils. In *First Results of the Second Phase of the “Short Term Action”*; Ispra JRC: Ispra, Italy, 2001.

Publisher’s Note: MDPI stays neutral with regard to jurisdictional claims in published maps and institutional affiliations.



© 2020 by the authors. Licensee MDPI, Basel, Switzerland. This article is an open access article distributed under the terms and conditions of the Creative Commons Attribution (CC BY) license (<http://creativecommons.org/licenses/by/4.0/>).